The Electronic Spectroscopy of 2,2′-Binaphthyl in Solution, Cryogenic Matrix and Supersonic Jet

Joanne L. Del Riccio, Fangtong Zhang, Anthony R. Lacey, and Scott H. Kable*

School of Chemistry, University of Sydney, Sydney, NSW, 2006 Australia

Received: January 12, 2000; In Final Form: June 7, 2000

The electronic spectroscopy of 2,2′-binaphthyl near 330 nm has been investigated by absorption spectroscopy in room-temperature solution and Shpolskii matrix at 4 K and by fluorescence excitation spectroscopy in a supersonic free-jet expansion. In the solution and gas phase, where the molecules are free to form the minimum-energy conformation, the spectra are quite different from those of 1,1′-binaphthyl and the parent naphthalene. However, when frozen in a matrix, aspects of the electronic spectrum resembled features of the spectra of these molecules. The fluorescence excitation spectrum in the free jet showed several long progressions in the torsional vibration with a characteristic, but anharmonic, frequency of about 30 cm^{-1}. The spectrum was assigned as the $1^1B \leftarrow 1^1A$ transition with an origin transition, which, although it could not be observed, was estimated to be at 30 060 ± 30 cm^{-1}. The frequency of 29 members of this progression allowed an accurate torsional potential to be calculated, which was flattened at low energy and approached harmonic at higher energy. The change in equilibrium torsional angle was estimated to be 32° upon electronic excitation, with the excited state being planar (either cis or trans). Several low-frequency vibrations were assigned in the gas phase that probably involve motions of the naphthalene structures as a whole about the central C−C bond. In the matrix, the torsional vibrations were frozen out, which allowed for the observation and tentative assignment of several higher-frequency vibrations resembling those of the bare naphthalene. The origin frequency was measured at 28 460 cm^{-1}. The difference between the gas-phase and solid-phase frequencies was attributed to the constrained structure of the molecule in the matrix.

I. Introduction

The spectroscopy and dynamics of bichromophoric molecules have been the subject of a great deal of research over several decades (see, for example, refs 1−3). The interest in these molecules and the motivation for such work stem from the desire to understand how two chromophores, located on a single molecule, interact. In some situations, these chromophores are strongly interacting. Yet in similar molecules or isomers, and even in the same molecule in different electronic states, they act independently. In some systems, the formation of a complex (e.g., a sandwich structure) is promoted when one or both of the chromophore moieties is electronically excited.

Biaryl species, where the chromophores are single and fused aromatic rings, have been used extensively for these investigations. The prototypical biaryl molecule is biphenyl, which has been the subject of numerous spectroscopic investigations.[4] These studies reveal that the molecule is planar in the solid state. In the gas phase, the rings are twisted by some 42°; however, upon electronic excitation, the molecule returns to near planarity.

Binaphthyl (BN) is the next simplest in this series of biaryl molecules, and yet, it has received much less attention. There are three isomers of BN, called 1,1′-binaphthyl (1,1′-BN), 1,2′-binaphthyl (1,2′-BN) and 2,2′-binaphthyl (see Table 1). The spectroscopy of these biaryls may or may not resemble that of their individual naphthalene chromophores, depending on the extent and type of interaction between the two ring systems.

TABLE 1: Chemical Structures and Abbreviations of the Molecules Referred to in This Paper

Molecule (abbreviation)	Structure	
Naphthalene	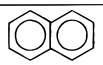	
1,1′-binaphthyl (1,1′-BN)	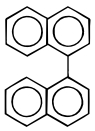 *cis* conformer	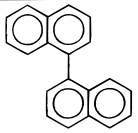 *trans* conformer
2,2′-binaphthyl (2,2′-BN)	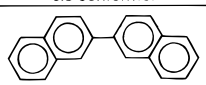 *cis* conformer	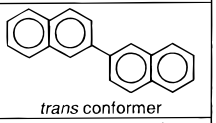 *trans* conformer
1,2′-binaphthyl (1,2′-BN)	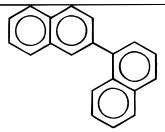 *cisoid* conformer	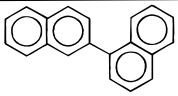 *transoid* conformer

Friedel et al. first studied the solution-phase UV electronic absorption spectra of all three BN isomers in 1948.[1] These spectra demonstrated a resemblance between the solution spectra of the naphthalene monomer and 1,1′-BN, whereas the absorption spectrum of 2,2′-BN was distinctly different (vide infra).

These results have been interpreted in terms of a subtle competition between resonance effects, which favor planarity, and steric hindrance, which favors more orthogonal structures. Together, these effects determine the conformations of the various isomers. The most relevant measure of conformation is

* Author to whom correspondence should be addressed. E-mail: s.kable@chem.usyd.edu.au.

10.1021/jp000166m CCC: $19.00
Published on Web 07/26/2000

the dihedral or torsional angle, θ, which is defined as the angle between the two planes of the naphthalene moieties. Absorption in the UV−visible region of the electromagnetic spectrum is due to a $\pi^* \leftarrow \pi$ transition. As the extent of π conjugation is one factor in determining conformation, perturbation of this conjugation by electronic excitation may have a large impact on the structure of these molecules.

1,1′-BN is the most sterically hindered of the BN's, with its two naphthyl groups forced out-of-plane by steric repulsions between the *ortho*-hydrogens that would occur in either planar conformation. When the naphthalene rings are perpendicular, there can be minimal overlap between the π systems on the two rings, so the naphthalenic nature of the π system on each moiety is retained with only slight perturbations. As the spectrum of 1,1′-BN was found to resemble that of naphthalene, Friedel et al. proposed that 1,1′-BN has a dihedral angle close to 90°.

In the case of 2,2′-BN, the proximity of the hydrogens in the planar conformation does little to offset the stabilization gained through increased π conjugation in a more planar form. Thus, 2,2′-BN is expected to adopt a more planar conformation than 1,1′-BN, resulting in π-electron delocalization across the whole molecule. Increased π-electronic communication between the two rings will lead to departures from a naphthalene-like spectrum.

The solution spectra of 1,1′-BN and 2,2′-BN are both red-shifted relative to the spectrum of naphthalene. This phenomenon reflects the tendency of biaryls to assume a more planar conformation in the excited electronic state than in the ground state. Because 2,2′-BN is red-shifted to a much greater extent, one would expect that its excited-state geometry would be closer to planar than that of 1,1′-BN and also, perhaps, that 2,2′-BN would undergo a greater change in conformation toward planarity on excitation. The torsional vibration in biaryls is of particular interest, as its measurement can yield information about how the dihedral angle of the molecule changes with electronic excitation.

Within the BN series, the spectroscopy of 1,1′-BN has been investigated most extensively, by experimental studies in solution, solid, low-temperature matrix, and supersonic expansion and by theoretical studies.[5−16] The jet-cooled laser-induced fluorescence (LIF) spectrum was interpreted in terms of a weakly coupled naphthalene dimer.[5,6] The spectrum displayed a weak origin region near 31 840 cm^{-1} and an intense false-origin region 437 cm^{-1} toward higher energy, which is characteristic of naphthalene. The shift of only ∼280 cm^{-1} between the $S_1 \leftarrow S_0$ origin(s) of 1,1′-BN and naphthalene indicated that there is little interaction between the two naphthalene rings. The torsional mode of 1,1′-BN was identified and measured to have a frequency of ∼30 cm^{-1}. From a Franck−Condon analysis, it was inferred that the excited-state torsional potential exhibits a double minimum. Thus, in the excited state, 1,1′-BN exists in two conformers: a cis-inclined conformer and a trans-inclined conformer (Table 1). The single minimum in the ground-state potential was assumed to be slightly cis of 90°. Upon excitation from the ground state, the dihedral angle was calculated to undergo a change of ∼12° to the trans side or ∼6° to the cis side to produce the two conformers. Semiempirical theoretical studies confirm these basic features.[12]

There are only a few spectroscopic studies of 2,2′-BN. Biraldi et al. have studied the fluorescence and absorption of 2,2′-BN in methanol solution.[17] From the fluorescence studies, it was established that 2,2′-BN exists as two conformers, a cis-inclined conformer and a trans-inclined conformer, in the ground state (Table 1). Both the fluorescence and the absorption spectra were resolved into two components corresponding to the contributions from each conformer. Other studies include a two-photon electronic absorption of 2,2′-BN in solution[18] and a femtosecond polarization study in solution that explored the intramolecular transfer of electronic excitation.[19]

The torsional potentials of many biaryls have been modeled or calculated by various theoretical techniques.[2,4,14−16,20−23] 1,1′-BN has been the subject of several of these studies.[12,14−16] Most recently, Biraldi et al. have calculated the torsional potential in the ground and first four excited singlet states by a semiempirical method (CS-INDO\CI).[7] These potentials seem promising, as they account for the majority of the observed spectroscopic behavior of 1,1′-BN in fluid and rigid solutions. However, this study does not appear to account for the jet-cooled molecular spectrum of 1,1′-BN. Contrary to the jet findings, Biraldi et al. failed to find a significant cis minimum in the first excited singlet state.

Biraldi et al. have also made CS-INDO\CI calculations of the torsional potentials of 2,2′-BN.[17] The ground electronic state (1^1A) and the first four excited electronic states (2^1A, 1^1B, 2^1B, and 3^1A) were determined to have double minima, again predicting the existence of cis-like and trans-like conformers. In the ground state, minima with similar energies occurred at $\theta \approx 35°$ and 145°. Excited-state potentials showed a move toward more planar configurations. (Within each excited state, the minima are separated in energy as well as in dihedral angle.) In the third excited state (2^1B), the cis conformation is markedly more energetically stable than the trans. A smaller and opposite effect occurs in the fourth excited singlet state (3^1A). Potentials for all states exhibit significant energy barriers to rotation through 90°. The torsional frequency of the ground state was calculated to be ∼40 cm^{-1}, while in the excited states, the torsional frequency varied from 30 to 40 cm^{-1}.

In the present study, we continue the investigation of the electronic spectroscopy of 2,2′-BN by repeating the solution-phase UV absorption spectroscopy of Friedel and recording the UV absorption spectra of 2,2′-BN in a Shpolskii matrix at 4 K[24] and the vapor-phase laser-induced fluorescence spectrum in a supersonic free-jet expansion.

II. Experimental Section

A. Solution Spectra. Absorption spectra of naphthalene, 1,1′-BN, and 2,2′-BN dissolved in a variety of solvents were collected at room temperature using a Cary 1E spectrophotometer. The scan rate was typically 20 nm/min with a slit width corresponding to 2.0-nm resolution. Solutions were prepared by dissolving crystalline samples in *n*-heptane. These solutions were placed in a quartz cell with a path length of either 1 or 5 cm. The sample concentration was prepared accurately and was varied from approximately 10^{-6} to 10^{-4} mol L^{-1} in order to capture all of the transitions in the ultraviolet/visible region.

B. Shpolskii Matrix Spectra. A Shpolskii matrix refers to a sample of organic compound dissolved and frozen in an *n*-alkane matrix.[24] Quasi-lines, which resolve vibrational structure, may result in the electronic spectrum of such a matrix. However, the appearance of these quasi-lines is dependent on the choice of solvent and sample concentration.[25] At present, there appears to be no way to predict which solvent or concentration will be optimal. As a result, the amount of sample and the length of the *n*-alkane chain must be varied until an adequately resolved spectrum is produced.

2,2′-BN was supplied by Kodak-Eastman and subsequently purified by recrystallization from A.R. benzene. The solvents,

n-heptane and *n*-pentane, were of spectroscopic purity. Both solvents were dried overnight with anhydrous calcium chloride immediately before use. Solutions of binaphthyl in *n*-alkane were prepared and degassed by a freeze−pump−thaw technique. The solution was sealed under vacuum in a quartz cell with a path length of approximately 1 mm.

Spectra were collected under two temperature conditions. For both temperature conditions, the sample must be frozen quickly to dissuade the *n*-alkane matrix from rejecting the binaphthyl. As slow freezing is required for the growth of a single crystal, a single crystal was not formed, and thus, no polarization data are available. Sample concentrations varied from 2×10^{-3} M for *n*-heptane to 1×10^{-2} M for *n*-pentane in solutions. Several concentrations were tried for *n*-heptane. However, it is difficult to know the exact concentration of sample in the *n*-alkane matrix. The matrix sometimes rejects the sample on freezing, and it appears that the sample concentration varies throughout the matrix.

Spectra taken at 4 K involve a nested pair of quartz dewars. The outer dewar is filled with liquid nitrogen. The inner dewar is then filled with liquid helium. A small region under vacuum separates the two dewars, and another evacuated region surrounds the nitrogen dewar. The liquid nitrogen and vacuum regions collectively serve to protect the inner dewar from heat exchange with the environment. The sample was frozen by immersion into liquid helium and remained in liquid helium while the spectra were taken. Spectra taken for *n*-heptane solutions utilized this method.

A flow-cell device was used to collect spectra at a temperature of ∼20 K. In this case, the sample cell is inserted into the quartz flow cell, which sits above a dewar of liquid helium so that vapor from the liquid helium can flow over the sample cell to freeze it. The temperature is decreased, and the flow rate increased, by boiling the liquid helium off by passing a small current through a wire-wound resistance immersed in the liquid helium. The outer compartment of the flow cell is again under vacuum. This method was used for the *n*-pentane solid solutions.

The sample was irradiated with light from a WOTAN XBO 150W/1 high-pressure xenon arc lamp. After passing through the sample, the light was focused onto the slit of a Hilger Littrow quartz spectrograph. The spectrograph dispersed the light, which was finally recorded photographically. The emission lines of an iron arc spectrum were used for wavelength calibration. After development, the film image was converted to a spectral trace using a Joyce-Loebl Mark IIIC microdensitometer.

C. Supersonic Free-Jet Spectra. 2,2′-Binaphthyl was supplied by Karl Industries Inc. (stated purity, 98%) and used as received. The sample was encased in a Nupro sintered filter holder, which was mounted directly behind a Precision Instruments pulsed nozzle. The sintered filter holder was heated to about 100 °C using Nichrome wire to ensure that enough BN was entrained in the expansion. The nozzle was heated to about 140 °C using a heater sleeve supplied by Precision Instruments to inhibit condensation of BN in the orifice. The temperature of the sample holder was monitored using a 100-Ω platinum-resistance thermometer attached to the top surface of the sample holder. Because 140 °C is close to the maximum rating of the nozzle (150 °C), the temperature of the nozzle was monitored using both a copper−constantan thermocouple inserted inside the heating sleeve and a 100-Ω platinum-resistance thermometer. Power supplied to both the Nichrome heating element and the heating sleeve was controlled independently by a homemade heating unit. The resistance of the thermometers was also converted directly to temperature and displayed by the unit.

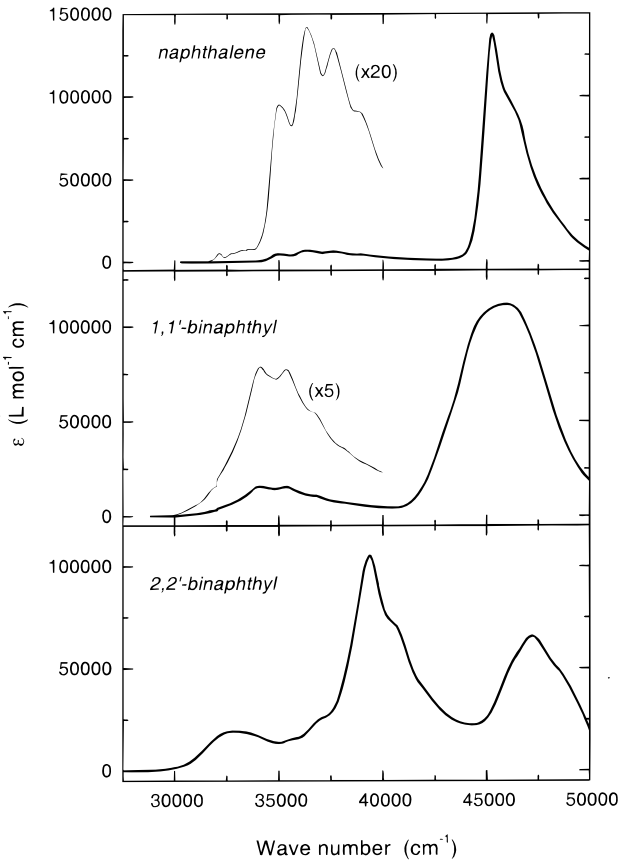

Figure 1. Solution spectra of naphthalene, 1,1′-binaphthyl, and 2,2′-binaphthyl.

Helium carrier gas was passed through the sample at pressures varying between 0.5 and 7 atm, although typically at 3 atm. The seeded gas undergoes a supersonic expansion in the vacuum chamber, via a 0.5-mm-diameter orifice in the pulsed nozzle. The nozzle is pulsed open at a repetition rate of 10 or 20 Hz. The expansion chamber is kept at a background pressure of below 10^{-6} mbar when the nozzle is not pulsing, maintained by a baffled Varian VHS-6 diffusion pump backed with an Alcatel 2033 mechanical pump.

The beam from an excimer-pumped dye laser (Lambda Physik Lextra-200 excimer and LPD-3001E dye laser) was directed into the vacuum chamber and made to intersect the jet 10 mm (X/D = 20) downstream from the nozzle. Two laser dyes were required to scan the 2,2′-BN spectrum. PTP (Exciton) dissolved in cyclohexane provided light in the range of 330−346 nm, and DCM (Exciton) produced light in the range of 304−332 nm after doubling in a KDP crystal. Fluorescence from binaphthyl molecules was collected with a photomultiplier (EMI 9789QB). The fluorescence signal was averaged by a Stanford SR250 boxcar integrator interfaced to a personal computer. Laser power was monitored with a photodiode and dye cuvette for normalization of all spectra.

Fluorescence lifetimes were measured after the 2,2′-BN was excited via several vibronic transitions. The delay between laser excitation and fluorescence collection was varied over consecutive laser pulses by scanning the boxcar gate to obtain a fluorescence decay curve.

III. Results

A. Solution Spectra. Figure 1 shows the spectra of naphthalene, 1,1′-binaphthyl, and 2,2′-binaphthyl in *n*-pentane solution. Each spectrum is a composite from at least three runs at

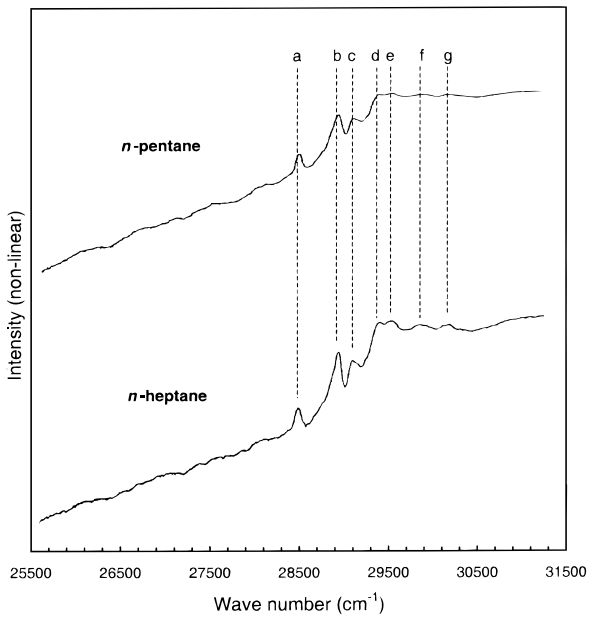

Figure 2. Electronic absorption spectra of 2,2′-BN in a Shpolskii matrix using either *n*-pentane (upper) or *n*-heptane (lower) as a solvent. Assignment of the peaks a−g is in Table 2.

different concentrations and path lengths, which were chosen so as to best measure the wide range of extinction coefficients for the different electronic transitions. These spectra are in quantitative agreement with those published by Friedel et al.[1]

The similarities between the spectra of naphthalene and 1,1′-BN are evident in the figure. Both naphthalene and 1,1′-BN exhibit an intense absorption band ($\epsilon > 10^5$) near 45 000 cm^{-1}. A weaker absorption band ($\epsilon \sim 7000$ for naphthalene and 15 000 for 1,1′-BN), containing some vibrational structure, is also evident in both spectra near 35 000 cm^{-1}. The weak ($\epsilon \sim 200$) vibronically induced $S_1 \leftarrow S_0$ transition of naphthalene is also seen near 32 000 cm^{-1}. 1,1′-BN has a similar $S_1 \leftarrow S_0$ transition, which has been observed in the supersonic free jet;[5,6] however, broadening in the solution spectra precludes its observation here.

In contrast, the 2,2′-BN spectrum does not resemble that of the parent naphthalene at all. Three prominent electronic transitions are apparent (32 500, 39 500, and 47 000 cm^{-1}) and perhaps another near 36 000 cm^{-1} that is partially obscured. Friedel et al. attributed the difference between the 1,1′-BN and 2,2′-BN spectra to the relative planarity of the 2,2′ species, which allows increased conjugation across the rings.[1] The 1,1′ species, on the other hand, is constrained sterically to having the rings perpendicular, thereby forbidding increased conjugation, and hence, to having an electronic structure similar to naphthalene.

B. Shpolskii Matrix Spectra. Figure 2 presents spectra of 2,2′-BN in *n*-heptane and *n*-pentane Shpolskii matrixes at 4 K. Several peaks are evident in both spectra. The frequencies for these transitions are displayed in Table 2. Although the calibration error for these spectra is ±5 cm^{-1}, extra error is introduced in estimating the center of these fairly broad absorption bands, giving a total uncertainty of ±10 cm^{-1}. The first prominent band occurs at approximately 28 459 cm^{-1}. A much more intense peak occurs about 440 cm^{-1} higher in energy. These two bands resemble the naphthalenic-origin/false-origin spacing, which leads us to consider the 28 459 cm^{-1} band as the electronic origin of 2,2′-BN and the 28 900 cm^{-1} band as corresponding to the vibronically induced naphthalenic false origin. The remaining bands can be assigned (Table 2) as either combinations or overtones of vibrations with frequencies of 440 and 612 cm^{-1} (a_1). The 612 cm^{-1} frequency is thought to be due to the C−C bond stretch between the two naphthalene moieties, which occurs at 651 cm^{-1} in the Raman spectrum of 2,2′-binaphthyl[26] and 681 cm^{-1} in the Raman spectrum of 1,1′-binaphthyl.[27]

TABLE 2: Spectral Line Positions of 2,2′-BN in *n*-Heptane and *n*-Pentane Shpolskii Matrices

	n-pentane		*n*-heptane		
label in spectrum	transition (cm^{-1})	difference (cm^{-1})	transition (cm^{-1})	difference (cm^{-1})	assignment
a	28 461	0	28 457	0	origin
b	28 898	437	28 901	444	440 (false origin)
c	29 072	611	29 071	614	612 (a_1)
d	29 368	907	29 350	893	2 × 440
e	29 503	1042	29 485	1028	440 + 612
f	29 821	1360	29 807	1350	3 × 440
g	30 117	1656	30 119	1662	440 + 2 × 612

The absolute uncertainty of these transitions is ±10 cm^{-1}.

C. Supersonic Free-Jet Spectra. A high-resolution laser-induced fluorescence (LIF) spectrum of the lowest-energy band is shown in Figure 3. A regular structure is very pronounced, exhibiting several long progressions in a very low-frequency vibration (∼30 cm^{-1}). This mode is assigned as the torsional vibration of the two naphthyl moieties about the C−C′ bond. The longest and most intense of these progressions is labeled with our estimate of the upper-state torsional quantum number, which is derived later. Four other progressions are labeled with a variety of different symbols. Table 3 lists the transition energies of the peaks labeled in the spectrum, separated by progressions, with our best estimate of the upper-state torsional quantum number, which is derived below. The symbols in the table header row correspond to the same symbols used to label the peaks in the figure. Another five progressions have been measured in part. However, increasing overlap between peaks at higher energies has made intensity measurements more difficult. As a consequence, assignment of the torsional quantum number for these progressions was far more difficult (see below), and they are listed separately in Table 4 with only very tentative torsional assignments ascribed to them. The absolute precision of the wavenumber values in Tables 3 and 4 is about 5 cm^{-1}, corresponding to the calibration uncertainty of our laser. The relative error, however, is only about 0.5 cm^{-1}.

A rising fluoresence background is apparent in Figure 3, which is probably due to spectral congestion. A lower-resolution, but extended, spectrum of 2,2′-BN is shown in Figure 4. It is a composite of two scans, necessitated by the need for changing laser dyes within the scan range. The rising fluorescence background is again apparent, embedded in which are several sharper features, again separated by 30 cm^{-1}. There is another structured region near 32 850 cm^{-1} and a broader diffuse region near 32 100 cm^{-1}. The sharp structure in the higher-energy region also shows several series of peaks separated by about 30 cm^{-1}. Although no evidence could be found for any transitions to the red of 30 000 cm^{-1}, we believe that the band system at 30 500 cm^{-1} is actually the vibronic false origin of the transition. Several features prompt us to make this assignment. First, if we were to consider this band to be the true origin, then the shift on going from vapor to solid solution would be about 1700 cm^{-1}. This figure is extraordinarily large when one considers that the same shift in 1,1′-binaphthyl is about 700 cm^{-1} and in naphthalene is only 960 cm^{-1} from vapor to crystal and about 460 cm^{-1} from vapor to mixed crystal. Second, the

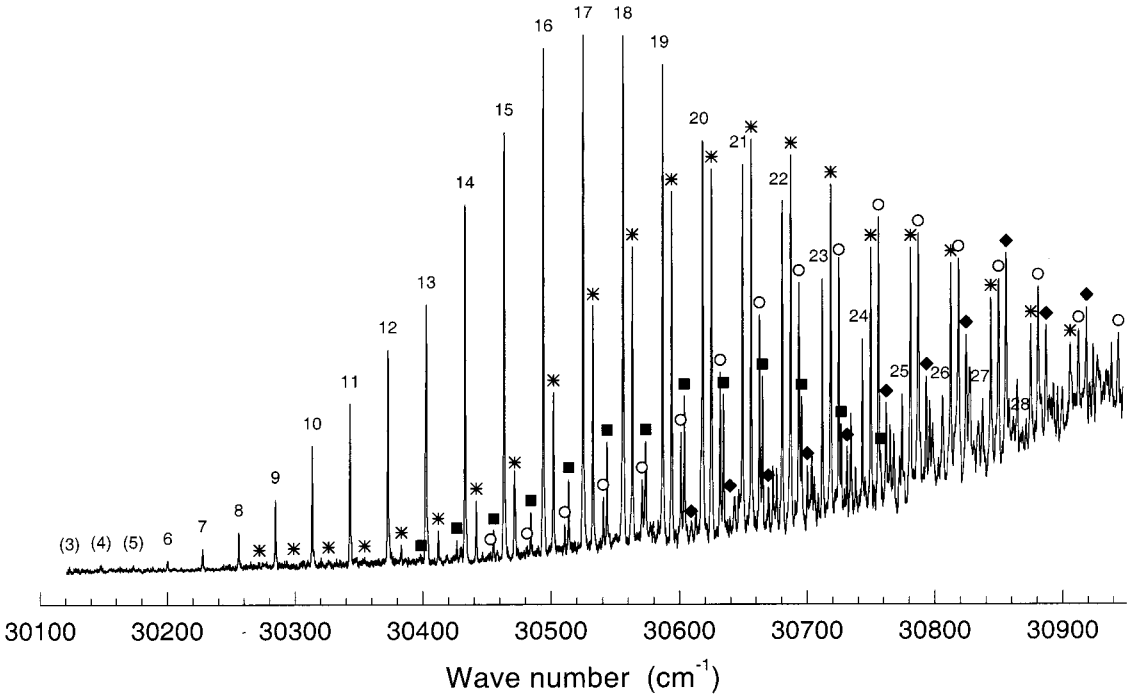

Figure 3. Laser-induced fluorescence spectrum of 2,2′-BN cooled in a supersonic expansion. The main, false-origin progression is labeled by the torsional quantum number, 3−28. Other progressions are indicated by symbols and assigned in Tables 3 and 4.

TABLE 3: Transition Energies (in cm^{-1}) of Peaks in the LIF Spectrum of Jet-Cooled 2,2′-BN[a]

v_{tors}[b]	prog. 1 origin	prog. 2 (★) +131 cm^{-1}	prog. 3 (■) +140 cm^{-1}	prog. 4 (○) +200 cm^{-1}
3	30 123.3			
4	30 148.1			
5	30 173.5			
6	30 200.3			
7	30 227.6	30 354.2		
8	30 255.9	30 383.1	30 398.5	
9	30 264.6	30 412.2	30 426.6	
10	30 313.4	30 441.8	30 455.3	30 510.7
11	30 342.9	30 471.5	30 484.3	30 540.6
12	30 372.6	30 501.9	30 513.7	30 570.7
13	30 402.7	30 532.5	30 543.5	30 601.1
14	30 433.1	30 563.2	30 573.5	30 631.9
15	30 463.6	30 593.9	30 603.8	30 662.6
16	30 494.1	30 625.0	30 634.4	30 693.6
17	30 525.0	30 656.1	30 665.0	30 724.9
18	30 556.0	30 687.2	30 695.7	30 756.0
19	30 586.9	30 718.6	30 726.8	30 787.0
20	30 618.1	30 749.9	30 757.5	30 818.6
21	30 649.4	30 781.0	30 788.8	30 849.8
22	30 680.5	30 812.4		30 880.7
23	30 711.9	30 843.7		30 912.4
24	30 743.4	30 874.9		30 943.9
25	30 774.4	30 905.9		
26	30 806.1			
27	30 837.3			
28	30 868.7			
29	30 899.5			

[a] The peaks are separated into progressions. Symbols associated with each progression correspond to the symbols placed over the peaks in Figure 3. [b] Error in labels is ±1.

TABLE 4: Transition Energies (in cm^{-1}) of Peaks in the LIF Spectrum of Jet-Cooled 2,2′-BN[a]

v_{tors} (tentative)	prog. 5 (★)	prog. 6	prog. 7	prog. 8
12	30 609.2	30 612.9		
13	30 639.5	30 643.1	30 646.2	
14	30 669.5	30 673.2	30 676.1	
15	30 700.2	30 703.6	30 705.6	
16	30 731.3	30 734.3	30 738.0	
17	30 762.0	30 765.0	30 768.0	
18	30 793.3	30 796.0	30 798.3	30 802.7
19	30 824.4	30 827.4	30 830.5	30 833.8
20	30 855.7	30 857.9	30 861.3	30 864.5
21	30 887.0			
22	30 918.9			
23	30 949.6			

[a] The peaks are separated into progressions. Symbols associated with each progression correspond to the symbols placed over the peaks in Figure 3. The upper-state torsional quantum number (v_{tors}) is only tentative in these cases.

similar false-origin band in 1,1′-BN (437 cm^{-1}) is 100 times stronger than the true origin,[5,6] which suggests that our experimental setup was not sufficiently sensitive to detect the true origin above the noise.

Finally, the range of the spectrum in Figure 4 encompasses known electronic transitions of naphthalene, 1,1′-BN, and 1,2′-BN. No features due to these molecules were found, indicating that the purity of the original sample was at least free from contamination from other isomers or from naphthalene itself.

1. Assignment of False-Origin Progression. The strongest progression (numbered in Figure 3) also extends furthest to the red, and we have consequently assigned this to a progression built on the false electronic origin. The progression intensity varies smoothly and symmetrically on each side of the maximum, which occurs near 30 525 cm^{-1}. In particular, the lack of a firm truncation to the progression at the red end makes assignment of the progression origin problematic. It is reasonable to imagine that the first members may be lost in the baseline noise or even that the first few members are hot bands. We varied the backing pressure between 1 and 4 atm to change the vibrational cooling in the expansion. The intensities of all peaks labeled "6" or greater were unchanged, and hence, they are believed to be cold bands. The intensities of peaks 3, 4, and 5 were variable; however, these are so close to our detection threshold that assignment of them as either "hot" or "cold" is uncertain. The labels are in parentheses to indicate such.

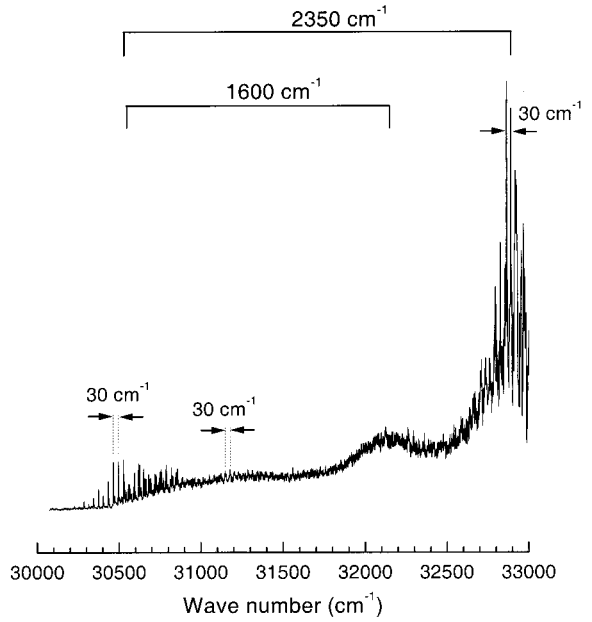

Figure 4. Lower-resolution, longer-range LIF spectrum of 2,2′-BN in a supersonic jet.

A one-dimensional Franck−Condon (FC) analysis was used to assist in locating the origin in the spectrum of 2,2′-BN. This analysis treats vibrations (torsions) in both the ground and excited electronic states as harmonic. As seen from Table 3, this is a reasonable approximation in the excited state where the first difference between transitions is fairly constant at 30 cm^{-1}, at least for higher vibrational levels. A recursion relation (derived from the harmonic oscillator recursion relations) involving two parameters is used to calculate the FC overlap integral for each transition in the progression.[28] The first parameter, D, is related to the change in normal coordinate between the ground and excited electronic states. The second parameter, δ, is related to the ground- and excited-state torsional frequencies by $\delta = (\upsilon''/\upsilon')$.[1/2]

The upper panel of Figure 5 shows the intensity distribution for all members of the origin progression. The idea of the FC analysis is to vary D and δ to obtain the best fit to the observed intensities. When D and δ are allowed to vary without constraint, however, a range of correlated values produce an acceptable fit, which provides a range of assignments. Thus, it was necessary to constrain the range of values that δ could take.

There is a trend among biaryl molecules (including biphenyl and 1,1′-BN) to favor more planar conformations in the excited state than in the ground electronic state.[7,20−23] Semiempirical calculations by Biraldi et al. suggest that this is also true for 2,2′-BN.[17] The closer the conformation is to planar, the greater is the double-bond character in the C−C′ bond, which in turn provides a larger force constant for the torsional motion. Thus, the excited-state torsional frequency is often greater than the ground-state frequency. We have therefore confined δ to values less than 1 (i.e., $\upsilon'' < \upsilon'$). Values of δ for two similar molecules, biphenyl-d_{10} (ref 4) and phenylcyclohexene,[21] are approximately 0.98, indicating that the torsional frequency does not change very much upon excitation. For the purposes of this exercise, we have constrained δ to lie between 0.85 and 1.0. D remains unconstrained.

Overlaid in Figure 5 is the resultant best FC fit to the observed intensities. The parameters that produced this fit were $\delta = 0.97$ (and therefore $\upsilon'' \approx 29$ cm^{-1}) and $D = 5.8$. The numbering that this analysis produces is shown overlaying Figure 3, with

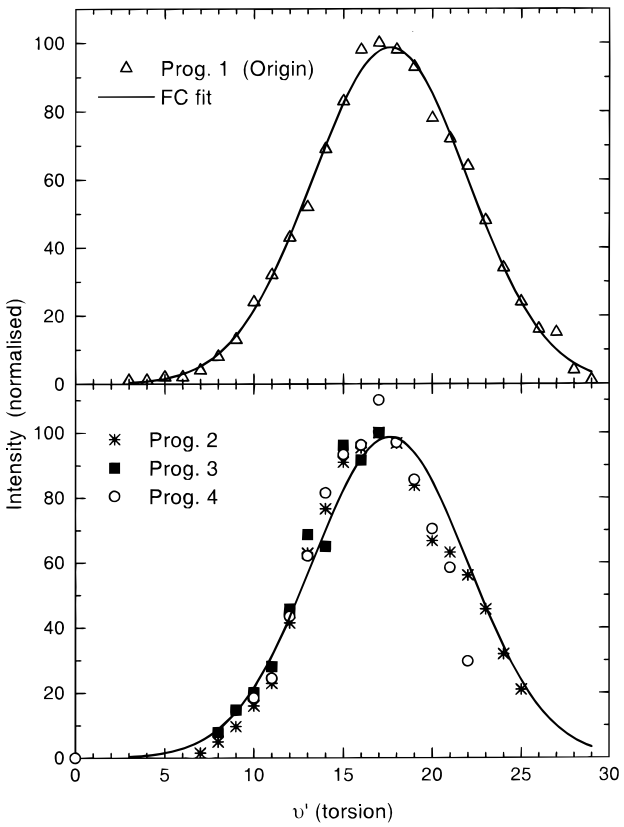

Figure 5. Intensity distribution of the strongest four torsional progressions. Symbols correspond to those in Figure 3. A one-dimensional Franck−Condon fit is shown as a solid line through the data.

the first definite cold-band assignment being the 6←0 transition and the maximum occurring for 17←0. The three tentative cold bands (labeled parenthetically 3−5) in fact fit the intensity pattern and so have been included in the table of assigned peaks (Table 3). The uncertainty in the fitting parameters (D and δ) produces an uncertainty in the numbering of ±1.

2. Assignment of Vibronic Progressions. The assignment of excited-state torsional quantum numbers to the other progressions in the 2,2′-BN spectrum suffers from the same problems as for the origin progression, even worse because the number of assigned peaks is smaller. However, providing that the torsional potential is similar for all progressions, the numbering can be made by comparison. There are two independent comparisons that can be made: the intensity distribution and the torsional frequency pattern.

The lower panel in Figure 5 shows the intensity distribution for three further torsional progressions, each based on a different false-origin transition (again symbols match those in the spectrum in Figure 3). The FC intensity distribution that best matched the origin progession is also shown as a solid line. The numbering of each progression was varied to best match the FC fit to the origin, and this best match is shown in the figure and in Table 3.

The upper panel of Figure 6 shows the first difference in the frequency of consecutive members of the origin progression. The plot shows a distinct rising trend with quantum number and, therefore, a negative anharmonicity. This is used in a later section to provide information on the torsional potential energy function. For the present purposes, however, its distinctive nature can be used to confirm the assignments of the torsional quantum numbers of the other false-origin progressions. This has been done in the lower panel of Figure 6, where the first differences

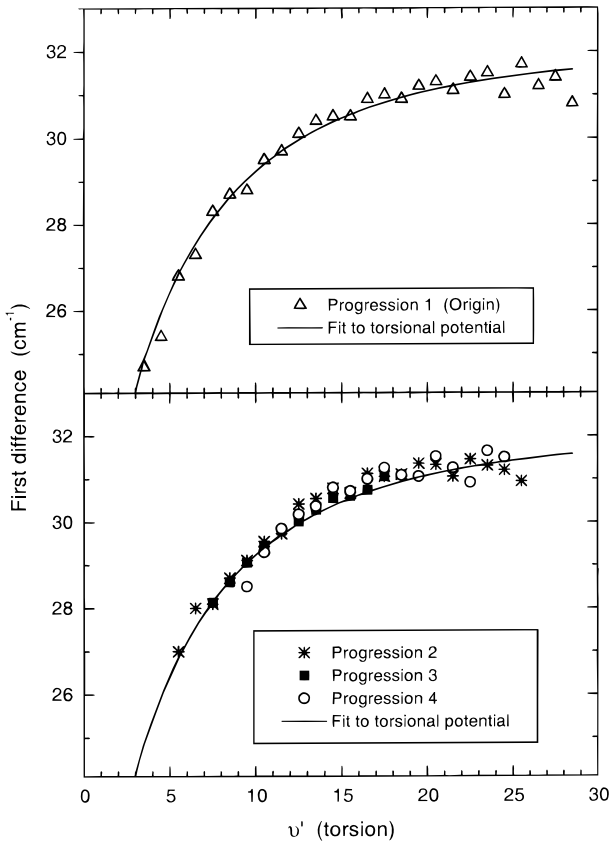

Figure 6. Energy difference between adjacent members of the first four torsional progressions. Symbols correspond to those in Figure 3. The calculated first difference for a model potential described in the text is shown as a solid line.

of the other three progressions have been plotted using the same quantum numbers as were inferred using the FC analysis. The match to the origin first difference trend is excellent, thereby supporting the assignment of quantum numbers and also confirming that the progressions all involve the same vibrational mode, an observation that takes on some importance when we consider later the number of electronic states and conformations of the molecule that may give rise to this electronic spectrum.

The shift in wavenumbers required to overlap each progression provides the vibrational frequency of the mode upon which the false origin progression is based. These three vibrational frequencies are calculated to be 131, 140, and 200 cm^{-1} for progressions 2−4, respectively. An uncertainty of ±30 cm^{-1} is again attributable to the above frequencies, as the assignments have an estimated error of $\Delta v = \pm 1$. Progressions 5−8 could not be assigned with any confidence by this method because increasing spectral overlap and decreasing intensity made intensity measurements inaccurate. These three low-frequency modes probably involve overall motion of the two naphthalene rings. There are six such inter-ring vibrations. The torsion has been assigned here, with a frequency of ∼30 cm^{-1}, and the inter-ring stretching vibration has been assigned previously[26] in the ground state as having a frequency of ∼650 cm^{-1}. Therefore, these three frequencies probably represent 3 of the 4 in-plane and out-of-plane bending vibrations. We are performing ab initio calculations of the excited state of 2,2′-BN to confirm these assignments and some other aspects of this work.

IV. Discussion

In this work, the electronic spectroscopy of 2,2′-binaphthyl has been measured in solution, cryogenic matrix, and free-jet expansion. The solution spectra confirm that the electronic states in 2,2′-BN are quite different from those in its parent naphthalene, which has been attributed previously to its more planar structure, thereby giving rise to increased π conjugation.[1] The supersonic jet spectra are dominated by long progressions in the torsional vibration, which indicate that there is a substantial change in equilibrium torsional angle upon electronic excitation. Several low-frequency modes were assigned, which probably involve in-plane and out-of-plane bends of the naphthalene moieties about the central C−C′ bond. In the cryogenic matrix, the torsional angle is frozen. Upon electronic excitation, it is unable to change to its new equilibrium angle, and hence, the long torsional progressions observed in the gas phase are also frozen out. This allows for the observation of other, higher-frequency vibrations, which are mostly assigned as naphthalene ring vibrations with frequencies very similar to those in the isolated naphthalene. In this section, we utilize the spectroscopic data to calculate a torsional potential, estimate the change in equilibrium torsion angle upon electronic excitation, and compare the 2,2′-BN results with those for other biaryl species and with theoretical calculations.

A. The Torsional Potential. Figure 6 shows that the spacing between torsional energy levels increases rapidly for small v and then levels out for $v > 15$ to a value of approximately 31 cm^{-1}. Thus, the torsional potential energy function must be fairly harmonic for large v but flatter than a quadratic function at low v. Eventually, of course, the potential energy must reach a maximum, which represents the barrier to isomerization between the cis and trans forms of 2,2′-BN. There is some evidence in Figure 6 that the spacing between levels is beginning to decrease at high v, and perhaps a slight alternation in the level spacing is appearing. However, the scatter in the data makes this conjecture fairly tenuous. The barrier would therefore seem to be much higher than the 1000 cm^{-1} (29 quanta) of the torsional potential probed in this work, and we have not tried to include a barrier in any of the model potentials that we tried.

Many authors have modeled torsional potentials using a sum of even cosine functions of the form

$$V(\theta) = {}^1/_2 \Sigma V_n (1 - \cos n\theta)$$

and obtained excellent fits to the torsional energy levels.[21,23] Similarly, we employed this potential function as a starting point. A generalized finite-element method (GFEM) was employed to model the one-dimensional torsional potential.[29] The GFEM method calculates the torsional energy levels for the potential function that is input into the program. We truncated the cosine series at terms of order six, but were unable to reproduce the experimental data in Figure 6. The best attempts could fit lower energy levels well, but were unable to reproduce the harmonic region of the potential. Undoubtedly, the inclusion of higher-order terms would improve the fit; however, the physical interpretation of such a function would be difficult.

Instead, we tried to model the potential using a quadratic function (which obviously fits the higher levels) that is flattened at the bottom by the addition of a Gaussian term. Such a potential has been used previously to model double-minimum potentials[22] and takes the form

$$V(\theta) = {}^1/_2 k\theta^2 + A \exp(-b\theta^2) \qquad (1)$$

A, b, and k are adjustable parameters, where A and b determine the amplitude and width of the Gaussian function, respectively, and k is the harmonic force constant. The best fit to the data in Figure 6 was obtained with values of $k = 4100$ cm^{-1} rad^{-2}, A

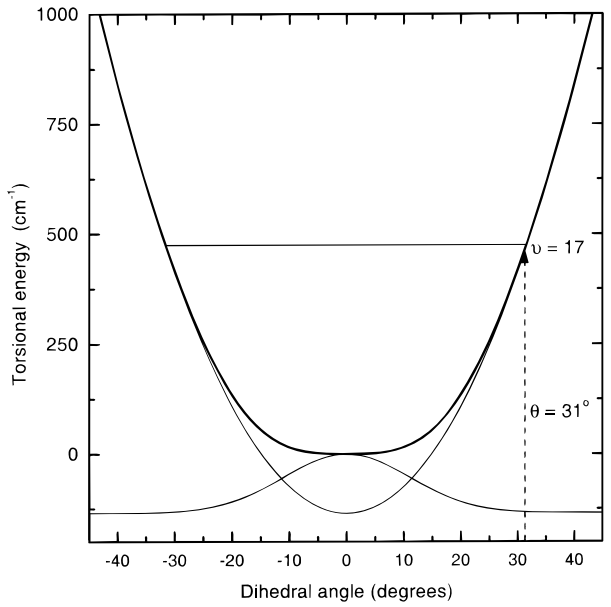

Figure 7. Model torsional potential for the excited state of 2,2′-BN. The energy of the $v = 17$ level, corresponding to the maximum Franck−Condon intensity, is shown, which enables an estimate of the ground-state equilibrium dihedral angle of 31° to be made.

$= 135$ cm^{-1}, and $b = 13.5$ rad^{-2}. Figure 7 displays the torsional potential that produced the best fit to the observed energy levels. This figure also shows the quadratic and Gaussian components that comprise the final function as lightweight lines.

The spacing between consecutive vibrational levels, which is calculated from this potential, is shown overlaying the experimental data in Figure 6 as a solid line and can be seen to represent the data well. There is an indication that the experimental values exhibit a greater flattening at higher quanta (maybe even starting to get smaller) than is achieved with the calculated values. This may indicate the approach of the region of the potential that begins to curve downward to form the isomerization barrier. This potential function in eq 1, of course, does not include any provision for a barrier.

The calculated torsional potential function can be used to extrapolate the energy level spacing to $v = 0$ and, hence, to derive an estimate of the electronic origin frequency. The origin position is estimated in this manner to occur at 30 060 cm^{-1} subject again to an error of about 30 cm^{-1}, which is derived from the ±1 uncertainty in the torsional assignments.

The change in dihedral angle that occurs upon excitation can also be estimated from the torsional potential and the FC analysis. The transition with maximum intensity in the progression occurs at $v' = 17$. The amplitude of vibration at this quantum number is approximately ±32°, as derived from the calculated potential function. A simple interpretation of the FC principle would then place this angle "vertically above" the ground-state equilibrium geometry; in other words, the change in equilibrium dihedral angle is 32° upon electronic excitation. The minimum energy in the excited state is 0° (trans-planar) or 180° (cis-planar), and the ground-state equilibrium dihedral angle, therefore, is 32° or 148°.

B. Assignment of the Electronic Transition. A sketch of the 2,2′-BN torsional potential energy surface is shown in Figure 8. The features are based on the semiempirical calculations (CS-INDO\CI) of Biraldi et al.[17] In the ground electronic state (1^1A), there are two, roughly equal-energy conformations, located about 35° out-of-plane from the cis and trans planar geometries. The rotational barriers to interchange of conformation, through either

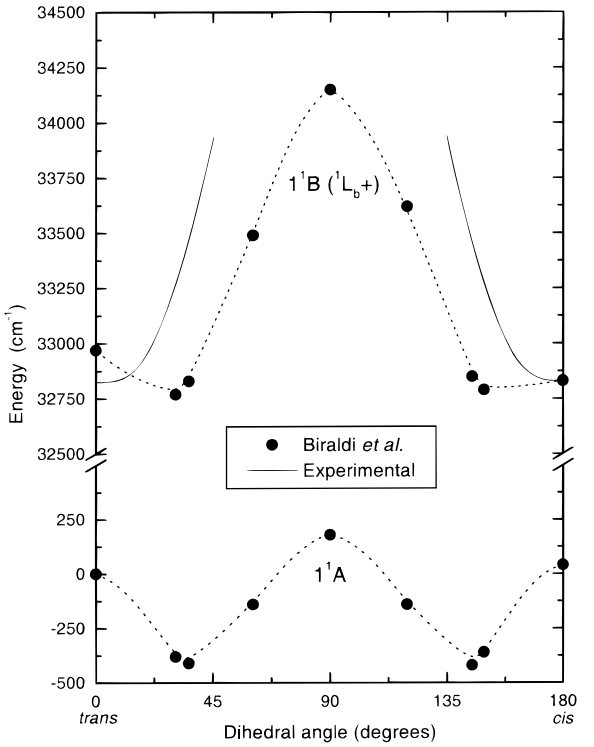

Figure 8. Calculated torsional potential for 2,2′-BN in the ground (1^1A) and excited (2^1B) states. The experimentally derived potential is also shown for the excited state.

0°, 90°, 180°, or 270°, are low. Therefore, it is likely that an ensemble of room-temperature gas- or solution-phase molecules would contain a statistical mixture of the two conformers. The solution spectra, therefore, would comprise absorption not only from both conformers, but also from a very wide range of inter-ring angles. In the cooled experiments, both gas-phase free jet, and solid Shpolskii matrix, it is likely that both conformers would be cooled into their respective torsional wells. In the matrix experiments, there are other factors that influence the conformation while freezing; however, we suspect that there should be no strong preference for either conformation. Consequently, in both experiments, there are potentially two conformers of 2,2′-BN that may give rise to the observed spectra.

The lowest-lying excited singlet electronic states of 2,2′-BN are the plus and minus dimer states corresponding to the ^{1}L$_b$ electronic state of naphthalene. These are labeled 2^1A [^{1}L$_b$(−)] and 1^1B [^{1}L$_b$(+)] and are degenerate when the rings are orthogonal. The oscillator strength for absorption to the 2^1A [^{1}L$_b$(−)] state has been calculated to be zero,[17] so we assign the activity in the spectrum to the 1^1B←1^1A transition, which is shown in Figure 8.

Only one distinct torsional progression (built on several false origins) was identified in the spectrum of jet-cooled 2,2′-BN. However, as reasoned above, there should be two rotational conformations of 2,2′-BN present in the sample, both of which will have their own characteristic potential energy surface and torsional vibronic structure. There are several possibilities that might give rise to only a single progression in the spectrum. (i) Only one conformer is populated, which we consider not likely, as discussed above, unless the calculated stability of each conformer is largely inaccurate. (ii) The torsional potential function is identical in both conformers, which would give rise to two different progressions that would be indistinguishable in the spectrum. This would seem quite unlikely, given the high

precision of the experimental measurements. (iii) The transition energy of the two conformers is different. The theoretical points plotted in Figure 8 show almost exact energy equivalence of the conformers in both electronic states. However, a difference of only about 300 cm^{-1} (<1 kcal/mol) would be sufficient for the higher-lying progression to be lost in the congestion of the lower transition (see Figure 3). This seems to us to be the most likely explanation.

The experimentally derived potential energy function from Figure 7 is plotted on top of the theoretical data points in Figure 8. The agreement is quite poor for both conformers (of course, we have only one experimental function). This poor agreement, coupled with the almost exact energy match for transitions in both conformers, makes it very difficult to confidently attribute the experimentally observed progressions to either of the conformers. We suspect the cis conformer, because the trans conformer is calculated to have an equilibrium geometry that is nonplanar, whereas the cis conformation is much more planar, in keeping with the experimental observation.

C. Other Vibrational Frequencies. In addition to the torsional vibration, which has been characterized above, several other excited state vibrations have been identified in the matrix and free-jet spectra. In the matrix, the large amplitude torsional vibration is frozen out, leaving higher-frequency modes more easily observed. One of these, with a frequency of 440 cm^{-1}, is so closely associated with the naphthalene vibronically inducing mode (ν_{44} in naphthalene)[30] that its assignment as the same mode in 2,2′-BN is firm. The other vibration is a progression-forming mode that is seen built on the origin and the false origin. It must, therefore, be a totally symmetric vibration. No naphthalene progression-forming mode has a similar frequency, and so, by analogy with the IR and Raman spectra of 2,2′-BN, we have assigned this mode as the dimer stretch with an excited-state frequency of ~612 cm^{-1}.

In the free jet, assignment of other vibrations relies on an accurate numbering of the torsional progression, with the frequency measurement being taken as the difference between the transition frequency of various progressions. This could be done fairly reliably for the first four progressions, listed in Table 3; however, the intensities of the progressions in Table 4 are affected too much by the increasing background congestion to be able to be assigned with any confidence. The four progressions in Table 3 correspond to the origin (probably the false origin) and three progressions displaced by 131, 140 and 200 cm^{-1}. Although naphthalene has a few vibrations with frequencies this low, these vibrations are not active in the naphthalene electronic spectrum. It would be unusual for them to be so dominant in the 2,2′-BN spectrum. Instead, we propose that these low-frequency vibrations are other dimer vibrations. The naphthalene dimer stretch ($\nu \sim 612$ cm^{-1}) and the torsion ($\nu \sim 30$ cm^{-1}) have been observed with significant Franck−Condon (FC) activity. Therefore, it seems plausible that other vibrations involving the two naphthalene rings will also exhibit FC activity in the spectrum. The four remaining dimer modes correspond to two in-plane bends (one in-phase and one out-of-phase) and two out-of-plane bends (again in- and out-of-phase). No calculations have been performed on these vibrations to aid our assignment; however, only two of these are totally symmetric and can, therefore, exhibit FC activity. The other two bending vibrations can only exhibit FC as even-quanta overtones, which are then also totally symmetric. Therefore, at least one of the assigned vibrational frequencies must, in fact, be an overtone frequency. The lowest-frequency dimer bend is likely to be the out-of-plane, in-phase motion (the "butterfly" mode). We believe that one of the 131 and 140 cm^{-1} vibrations is probably two quanta of this vibration, and hence, the "butterfly" vibration probably has a frequency of ~70 cm^{-1}. An excited-state normal-coordinate analysis will probably be the most useful tool for securing these assignments. Our assignment of various excited-state frequencies is summarized in Table 5.

TABLE 5: Vibrational Assignments in the 1^1B State of 2,2′-BN

frequency (cm^{-1})	assignment
31	dimer torsion
131 and/or 140	$2 \times \sim 70$ cm^{-1} (butterfly) or dimer bend
200	dimer bend or 2×100 dimer bend
440	naphthalene ring mode, equivalent to ν_{44} in naphthalene (ref 30)
612	dimer stretch

V. Conclusions and Future Work

In this work, we have measured the electronic spectroscopy of 2,2′-binaphthyl in solution, Shpolskii matrix, and supersonic free jet. The molecule is planar in the excited state and ~32° out-of-plane in the ground state, although it could not be determined which of the cis and trans conformers was active in the spectrum. In the matrix, the electronic origin was found at 28 460 cm^{-1}. The stronger naphthalene-like false origin was 440 cm^{-1} higher in frequency. In the gas phase, the false origin was assigned at 30 060 cm^{-1}, while the true origin was too weak to be observed. A long progression in the torsional vibration (30 cm^{-1}) was observed in the gas-phase spectrum, which allowed a detailed characterization of the torsional potential. The experimentally derived potential is in poor agreement with previous theoretical calculations. Other strong progressions, involving the other dimer vibrations, were also present in the spectrum. Assignment of these was difficult, however, as there is activity in at least 5 of the 6 dimer modes in the spectrum.

We are performing ab initio theoretical calculations on the ground and excited states of 2,2′-BN in an attempt to assign the FC-active vibrations in the free-jet spectrum. We will also recalculate the torsional potential to explore whether better agreement with the experimentally derived potential can be obtained. Finally, we hope that these more extensive calculations will provide insight as to why only one torsional progression was observed in the free-jet spectrum.

Acknowledgment. We gratefully acknowledge the receipt of an ARC (small) grant to support this research. We thank Dr. George Bacskay for insight into the 2,2′-BN potential energy surface and for providing the GFEM code. We also thank Dr. Ondrej Votava for experimental assistance at various stages of this project.

References and Notes

(1) Friedel, R. A.; Orchin, M.; Reggel, L. *J. Am. Chem. Soc.* **1948**, *70*, 199.
(2) Hochstrasser, R. M. *Can. J. Chem.* **1961**, *39*, 459.
(3) Ito, M. *J. Phys. Chem.* **1987**, *91*, 517.
(4) Takei, Y.; Yamaguchi, T.; Osamura, Y.; Fuke K.; Kaya, K. *J. Phys. Chem.* **1988**, *92*, 577.
(5) Jonkman, H. T.; Wiersma, D. A. *Chem. Phys. Lett.* **1983**, *97*, 261.
(6) Jonkman, H. T.; Wiersma, D. A. *J. Chem. Phys.* **1984**, *81*, 1573.
(7) Riley, M. J.; Lacey, A. R.; Sceats, M. G.; Gilbert, R. G. *Chem. Phys.* **1982**, *72*, 83.
(8) Lacey, A. R.; Craven, F. J. *Chem. Phys. Lett.* **1986**, *126*, 588.
(9) Hara, Y.; Nicol, M. F. *Bull. Chem. Soc. Jpn.* **1978**, *51*, 1985.
(10) Shank, C. V.; Ippen, E. P.; Teschke, O.; Eisenthal, K. B. *J. Chem. Phys.* **1977**, *67*, 5547.
(11) Tetreau, C. *J. Phys. Chem.* **1986**, *90*, 4993.

(12) Biraldi, I.; Ponterini G.; Momicchioli, F. *J. Chem. Soc., Faraday Trans. 2* **1987**, *83*, 2139.
(13) Gamba, A.; Rusconi, E.; Simonetta, M. *Tetrahedron* **1970**, *26*, 871.
(14) Post, M. F. M.; Eweg, J. K.; Langelaar, J.; van Voorst, J. D. W.; ter Maten, G. *Chem. Phys*. **1976**, *14*, 165.
(15) Post, M. F. M.; Langelaar, J.; van Voorst, J. D. W. *Chem. Phys. Lett.* **1975**, *32*, 59.
(16) Gustav, K.; Suhnel, J.; Wild, U. P. *Chem. Phys*. **1978**, *31*, 59.
(17) Biraldi, I.; Bruni, M. C.; Caselli, M.; Ponterini, G. *J. Chem. Soc., Faraday Trans. 2* **1989**, *85*, 65.
(18) Druker, R. P.; McClain, W. M. *Chem. Phys. Lett.* **1974**, *28*, 255.
(19) Zhu, F.; Galli, C.; Hochstrasser, R. M. *J. Chem. Phys.* **1993**, *98*, 1042.
(20) Zgieski, M. Z.; Zerbotto, F.; Shin, Y.-D.; Lim, E. C. *J. Chem. Phys.* **1992**, *96*, 7229.
(21) Finlay, J. P.; Cable, J. R. *J. Phys. Chem.* **1993**, *97*, 4595.
(22) Chakraborty, T.; Lim, E. C. *J. Chem. Phys.* **1993**, *98*, 836.
(23) Werst, D. W.; Brearley, A. M.; Gentry, W. R.; Barbara, P. F. *J. Am. Chem. Soc.* **1987**, *109*, 32.
(24) Shpolskii, E. V. *Sov. Phys. Usp.* **1963**, *6*, 411.
(25) Dekkers, J. J.; Hoornweg, G. P.; MacClean, C.; Velthorst, N. H. *J. Mol. Spectrosc.* **1977**, *68*, 56.
(26) Wynne-Jones, D. *Honours thesis*, University of Sydney, Sydney, NSW, Australia, 1992.
(27) Hurst, J. *Honours thesis*, University of Sydney, Sydney, NSW, Australia, 1991.
(28) Henderson, J. R.; Muramoto, M.; Willett, R. A. *J. Chem. Phys.* **1964**, *41*, 580.
(29) Nordholm, S.; Bacskay, G. B. *Chem. Phys. Lett.* **1976**, *42*, 253.
(30) Craig, D. P.; Hollas, J. M. *Philos. Trans. R. Soc. London* **1961**, *253*, 569.